This article has been accepted for publication in a future issue of this journal, but has not been fully edited. Content may change prior to final publication. Citation information: DOI 10.1109/TAP.2018.2867024, IEEE Transactions on Antennas and Propagation

What is the problem that is addressed by the manuscript, and why is it important to the Antennas Propagation community? (limited to 100 words).

Circularly polarized (CP) horn antennas play an important role in many applications, such as satellite and communication, radio astronomy, as well as radar systems. However, the millimeter-wave CP horn always has a high processing cost. This communication proposed a new type of wideband low-cost CP horn antennas with no requirement of orthogonal mode transducer (OMT) feeding.

The CP working principle of the proposed prototype was explained. A series of parametric studies were carried out to provide the guideline for this type CP horn.

What is the novelty of your work over the existing work? (limited to 100 words).

Compared with the CP antenna horn fed by a type of creating grooves or irises' waveguide polarizers, the proposed antenna has an approximately equivalent operating bandwidth, a lower cost, and a simpler structure. Compared with CP horn fed by filling dielectric-type waveguide polarizers, this antenna has lower cost and better shock resistance. In addition, unlike the above-mentioned two types of waveguide polarizer, this antenna does not need the OMT feeding. Compared with a CP horn fed by a septum polarizer, this antenna has a wider axial-ratio (AR) bandwidth and symmetrical radiation pattern.

Provide up to three references, published or under review, (journal papers, conference papers, technical reports, etc.) done by the authors/coauthors that are closest to the present work. Upload them as supporting documents if they are under review or not available in the public domain. Enter "N.A." if it is not applicable.

Y. Yao, X. Cheng, J. Yu, and X. Chen, "Analysis and design of a novel circularly polarized antipodal linearly tapered slot antenna," *IEEE Trans. Antennas Propag*., vol. 64, no.10, pp. 4178-4187, Oct. 2016.

Y. Yao, X. Cheng, J. Yu, and X. Chen, "Wideband circularly polarized antipodal curvedly tapered slot antenna array for 5G applications," *IEEE J. Sel. Areas Commun*., vol .35, no. 7, Jul. 2017.

Provide up to three references (journal papers, conference papers, technical reports, etc.) done by other authors that are most important to the present work. Enter "N.A." if it is not applicable.

Y. Liu, H. Lu, Y. Wu, M. Cui, B. Li, P. Zhao, and X. Lv, "Millimeterwave and terahertz waveguide-fed circularly polarized antipodal curvedly tapered slot antennas," *IEEE Trans. Antennas Propag*., vol. 64, no.5, pp. 1607-1614, May. 2016.

This article has been accepted for publication in a future issue of this journal, but has not been fully edited. Content may change prior to final publication. Citation information: DOI 10.1109/TAP.2018.2867024, IEEE Transactions on Antennas and Propagation

Analysis and Design of a Low-Cost Circularly Polarized Horn Antenna

Xiaohe Cheng, *Student Member, IEEE,* Yuan Yao, *Senior Member*, *IEEE*, Tao Yu, Zhijiao Chen, *Member*, *IEEE*, Junsheng Yu, and Xiaodong Chen, *Fellow*, *IEEE*

***Abstract*— A millimeter-wave wideband circularly polarized (CP) horn antenna with no requirement of an orthogonal mode transducer (OMT) feeding is reported. The horn antenna has a simple structure, which consists of an antipodal curvedly tapered slot antenna and a circular waveguide. The CP principle of the horn is explained. A series of parametric studies were carried out to estimate the effect of key parameters, and the design procedure is also presented. The measured results are in reasonable agreement with the simulated results. The experimental results indicate that the proposed antenna can achieve a bandwidth of 40% (50–75 GHz) for both the axial ratio (AR) < 3.2 dB and the reflection coefficient S_{11} < -10 dB. The proposed antenna is easy to manufacture and is a good candidate for the low-cost wideband CP horn antenna.**

***Index Terms*— circularly polarized antenna, horn antenna, millimeter-wave, slot line**

I. Introduction

Circularly polarized (CP) horn antennas play an important role in many applications, such as satellite communication, radio astronomy, as well as radar systems [1], which can achieve better polarization efficiency and reduce multipath propagation effects [2]. A representative CP horn antenna basically consists of a circular polarizer and a horn antenna [3]. The polarizer is the critical component in the CP horn antenna's design, which is responsible for converting linearly polarized (LP) waves to CP waves.

Various waveguide polarizers have been proposed to feed the horn antenna in previous research, and can be divided into three groups. The first group is represented by creating grooves [4] or irises [5] on the waveguide wall to achieve a 90° phase difference between the two orthogonal modes. This type of polarizer attains a high-strength structure, a wide bandwidth and a low loss. However, high-precision processing techniques are necessary in fabricating grooves and irises. The cost of this type of polarizer would be further raised with the increase in operating frequency owing to the correspondingly decreasing size. The second group is realized by filling dielectric plates in the waveguide. Filling the dielectric stab in the sidewall or at the center of the waveguide was proposed in [6] & [7]. This type of polarizer also has a wide operating bandwidth, but it is not suitable for a violent vibration working environment and also has high processing-technology requirements. Moreover, its dielectric loss in the high-frequency band could not be ignored either. Furthermore, these two types of polarizer require the orthogonal mode transducer (OMT) to supply the two equiphase orthogonal modes [8].

The last group is the septum polarizer, which is more compact in size, since it does not require the OMT, compared to the above-motioned polarizers. Its typical structure comprises a metal septum at the center of a square waveguide [9]. The analysis of the thickness and shape of the septum were carried out in [10] & [11], and it is easy to achieve dual polarization characteristic. These designs are simple, but their asymmetrical structures would impair the overall performance of horn antennas. For instance, the radiation patterns of the CP horn antenna proposed in [3] & [12] were asymmetrical, and the 3 dB axial-ratio (AR) bandwidths are relatively narrow (less than 20%) since it is difficult to control the rotation of the *x*- and *y*-polarizations simultaneously in both magnitude and phase. In particular, the square waveguide polarizers are easy to model and optimize, but they also require a transition from a square to a circular waveguide to connect to the circular horn antenna.

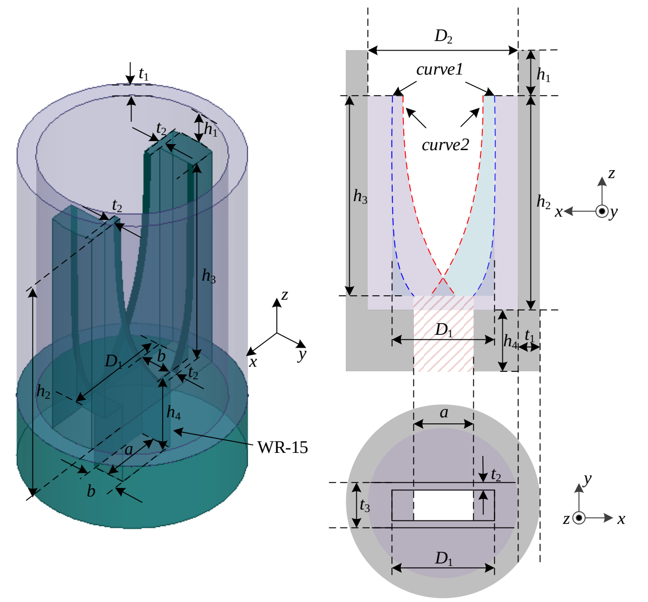

Fig. 1. Configuration of the proposed antenna.

To address the problems above, in this communication, a new type of CP horn is proposed, in which an antipodal tapered slot antenna (ATSA) [13]–[15] is inserted in the circular waveguide. The proposed structure inherits the advantage of the sample structure of the septum polarizer, and its AR bandwidth is significantly enhanced owing to the symmetric structure. The dual polarization characteristic of the septum polarizer was cancelled, but the proposed antenna benefits from the balanced structure and consequently has a symmetrical radiation pattern in *x*-*z* and *y*-*z* plane, respectively. The proposed antenna achieves a measured bandwidth of 40% for both AR < 3.2 dB and reflection coefficient S_{11}< -10 dB. A measured gain of 12.21 ± 2.4 dBic was achieved from 50 to 75 GHz.

Manuscript received on December 29, 2017. This work was supported by the National Natural Science Foundation of China under Grant No. 61474112, in part by the BUPT Excellent Ph.D. Students Foundation under grant CX2017304, in part by the China Scholarship Council.

Xiaohe Cheng, Yuan Yao, Zhijiao Chen and Junsheng Yu are with the Beijing Key Laboratory of Work Safety Intelligent Monitoring, Beijing University of Posts and Telecommunications, Beijing, 100876, China (corresponding author's e-mail: yaoy@ bupt.edu.cn).

Tao Yu is with the Department of Electrical and Electronic Engineering, Tokyo Institute of Technology, Tokyo 152-8552, Japan.

Xiaodong Chen is with the School of Electronic Engineering and Computer Science, Queen Mary University of London, London, UK.

II. Antenna Design

A. Geometry

The geometry of the proposed wideband CP horn antenna is

This article has been accepted for publication in a future issue of this journal, but has not been fully edited. Content may change prior to final publication. Citation information: DOI 10.1109/TAP.2018.2867024, IEEE Transactions on Antennas and Propagation

TABLE I
OPTIMIZED ANTENNA DESIGN DIMENSIONS

Parameter	t_1	t_2	t_3	a	b	D_1
Value (mm)	1	0.41	2.7	1.88	3.795	6.6
Parameter	D_2	h_1	h_2	h_3	h_4	W_0
Value (mm)	10	2	13.9	13	4.1	0.85
Parameter	W_1	W_2	W_3	Q_1	Q_2	
Value (mm)	2.6	2	3.3	0.4	0.75	

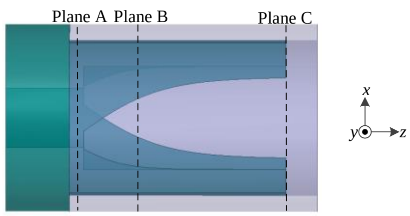

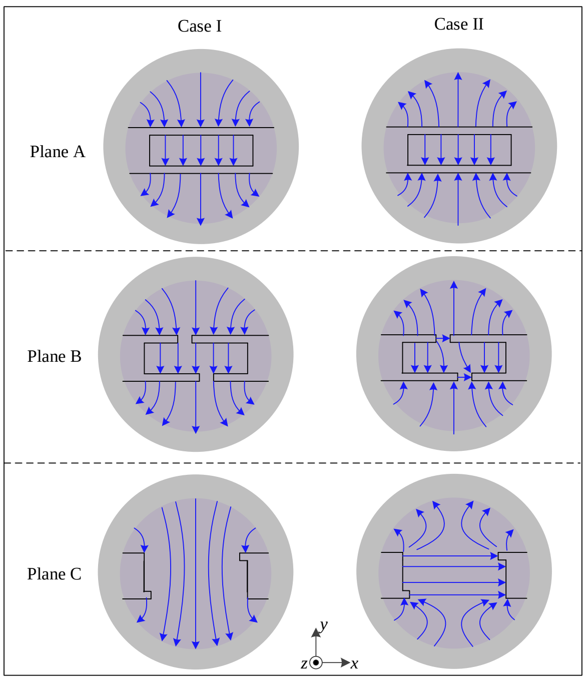

Fig. 2. Illustration of the electric field distributions at Planes A, B and C in case I and case II.

illustrated in Fig. 1, in which an ATSA is filled in the center of the circular waveguide with diameter D_2, thickness t_1 and length $h_1 + h_2$. The ATSA consists of a WR-15 waveguide and a widened waveguide (the x-direction widens from a to D_1). The broad wall of the widened waveguide has two symmetrical slots. As the original point is specified in Fig. 1, the slots' curves are defined by

$$Curve1: x_1(z) = \pm\left(\frac{2(W_0+W_1)}{1+e^{-Q_1 z}} - 2W_0 - W_1\right) \tag{1}$$

$$Curve2: x_2(z) = \pm\left(\frac{2(W_2-W_3)}{1+e^{-Q_2 z}} - 2W_2 + W_3\right)$$

The accurate dimensions of the proposed antenna are presented in Table I.

B. Mechanism Analysis

For the generation of the CP wave, the critical aspect is to simultaneously achieve a low amplitude difference and a 90° phase shift between the two orthogonal electric field components. Due to the symmetry of the proposed horn structure, two imaginary ports with the same input power are placed at the up and down sides of the

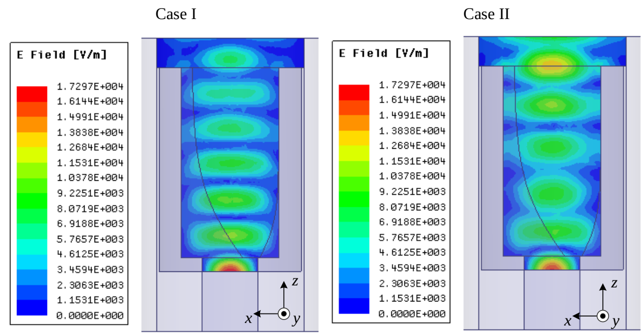

Fig. 3. Illustration of the electric field distributions at x-z plane of proposed horn with input electric fields distribution as shown in case I and case II.

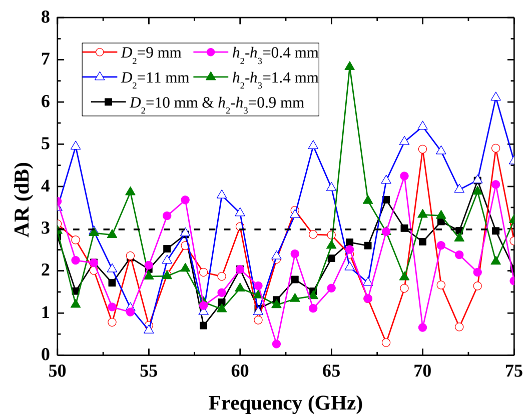

Fig. 4. Comparison of simulated AR plots at the boresight with different circular waveguide diameters D_2 and back-cavity lengths $h_2 - h_3$.

WR-15 waveguide, as shown in Fig. 2. It should be noted that the input phases of imaginary ports are the same in case I and contrary in case II. When the WR-15 port is excited, the input electric fields can be equalized as the superposition of the fields in case I and case II, as illustrated in the electric fields in the Plane A of Fig. 2. In case I, similar to the even mode coupling mechanism in waveguide septum polarizer [9], the electric fields have the same directions in the rectangular waveguide and in the surrounding circular arc waveguide. The currents on two sides of the two broadsides of the rectangular waveguide have opposite directions. Thus, as the wave transmits to Planes B and C, the slots on the broadside of the rectangular waveguide would not disturb the field. When the electromagnetic wave is transmitted to the antenna aperture, the amplitude of the x-direction electric field (E_x) is small which is generated by the circular waveguide modes. In case II, the electric fields have opposite directions in the rectangular waveguide and the surrounding arc waveguide. Thus, the electric fields will be disturbed by the slots. The amplitude of the x-direction electric field increases gradually with the electromagnetic wave transmitting to the antenna aperture, as shown in case II in Fig. 2. By optimizing the parameters of the slot reasonably, a low amplitude difference of the orthogonal electric fields can be obtained. The different cross-sectional dimensions of a waveguide guide the electromagnetic wave at different wavelengths with the same frequency [16]. Fig. 3 shows the electric fields distribution at x-z plane of the horn with the input electric fields distribution, as shown in case I and case II. As the wave transmits to the aperture, the phase difference between the E_x

This article has been accepted for publication in a future issue of this journal, but has not been fully edited. Content may change prior to final publication. Citation information: DOI 10.1109/TAP.2018.2867024, IEEE Transactions on Antennas and Propagation

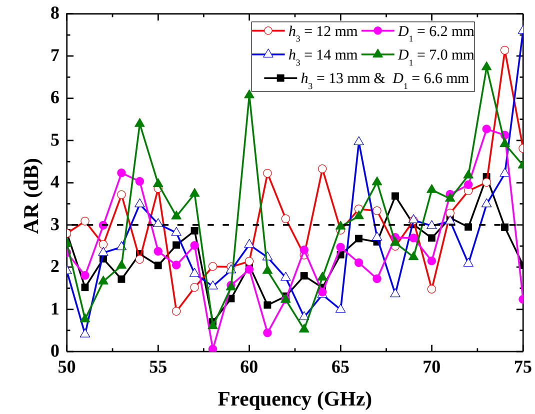

Fig. 5. Comparison of simulated AR plots at the boresight with different slot lengths h_3 and broadened waveguide widths D_1.

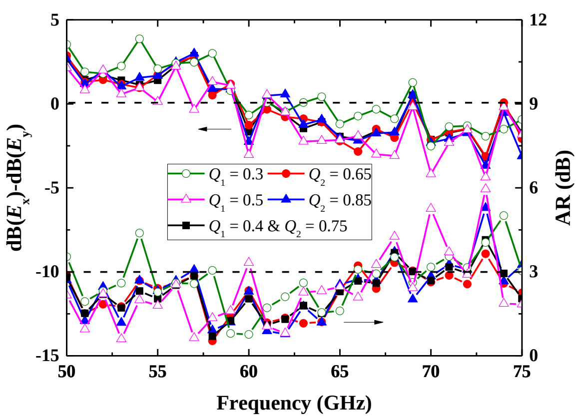

Fig. 6. Comparison of a simulated amplitude difference of the orthogonal electric field (dB(Ex) – dB(Ey)) in the far field at the boresight with different slot curvatures Q_1 and Q_2.

and y-direction electric field (E_y) is around -90°, and the LHCP wave is generated. By optimizing the width of broadened waveguide D_1 and the diameter of circular waveguide D_2 to control the reasonable wavelength and adjust the guide structure length h_2, the 90° phase shift can be achieved.

C. Parameter Study

The operating mechanism of the proposed CP horn antenna has been analyzed in Section B. A series of parametric studies were employed to discuss the effect of AR performance of this horn antenna. The value of the circular waveguide diameter D_2 would affect the guide wavelengths in case I and case II, and the amplitude E_x and E_y. As illustrated in Fig. 4, when D_2 equals to 11 mm, the CP property deteriorates significantly. Besides, the shape and length of the back cavity is also an important indicator that affects the antenna performance [3]. For the convenience of processing, the authors simply optimize the length of back cavity $h_2 - h_3$ without any curve shape. The length of slots h_3 has an effect on the mode coupling. As illustrated in Fig. 5, when the value of h_3 equals to 12 or 14 mm, the coupling effect is not satisfied, this increases the value of AR. The width of widened waveguide D_1 is also an important parameter to the guide wavelength of the even and odd modes. The influence of D_1 is

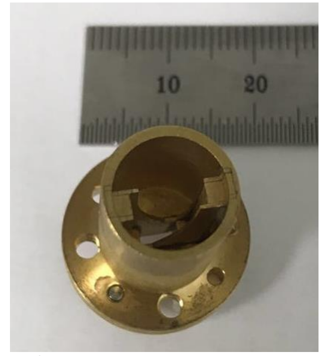

Fig. 7. A photograph of the proposed CP horn antenna.

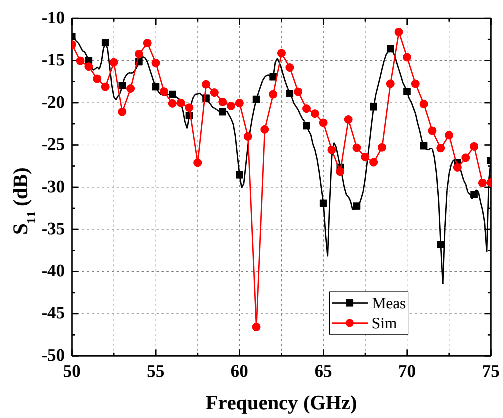

Fig. 8. Measured and simulated reflection coefficients of the proposed CP horn antenna.

also illustrated in Fig. 5. To obtain the low amplitude difference of E_x and E_y, it is necessary to adjust the curvatures of the slots Q_1 and Q_2. As illustrated in Fig. 6, the difference of the amplitude of the E_x and E_y in the far field increases with the decrease in Q_1. The value of Q_2 is used to fine-tune the CP property. In conclusion, through tuning these parameters, a desired CP performance of the proposed antenna can be achieved.

D. Design Procedure

Step 1): Choosing the standard rectangular waveguide to feed the antenna according to frequency requirements.

Step 2): Modeling the ATSA and adjusting the value of D_1 to achieve the initial 90° phase differences between E_x and E_y in the far field without considering the amplitude of E_x and E_y.

Step 3): Placing the optimized ATSA at the center of the circular waveguide, adjusting D_1, D_2, h_2, and h_3 to obtain the preliminary simulation results, optimizing Q_1 and Q_2 to obtain the low amplitude difference of E_x and E_y in the far field.

Step 4): Checking if the phase difference between E_x and E_y is located within the available range. If so, the antenna design is completed; if not, optimizing D_1, D_2, h_2 and h_3.

III. Simulated and Measured Results

The proposed CP horn antenna was fabricated by a conventional wire-cutting electrical discharge machine (EDM). The prototype of the proposed CP horn antenna is illustrated in Fig. 7. The S-parameter of the CP horn was measured with an Agilent Network Analyzer E8361A, and its AR, gain and radiation pattern were measured by a millimeter-wave compact antenna test range (CATR).

This article has been accepted for publication in a future issue of this journal, but has not been fully edited. Content may change prior to final publication. Citation information: DOI 10.1109/TAP.2018.2867024, IEEE Transactions on Antennas and Propagation

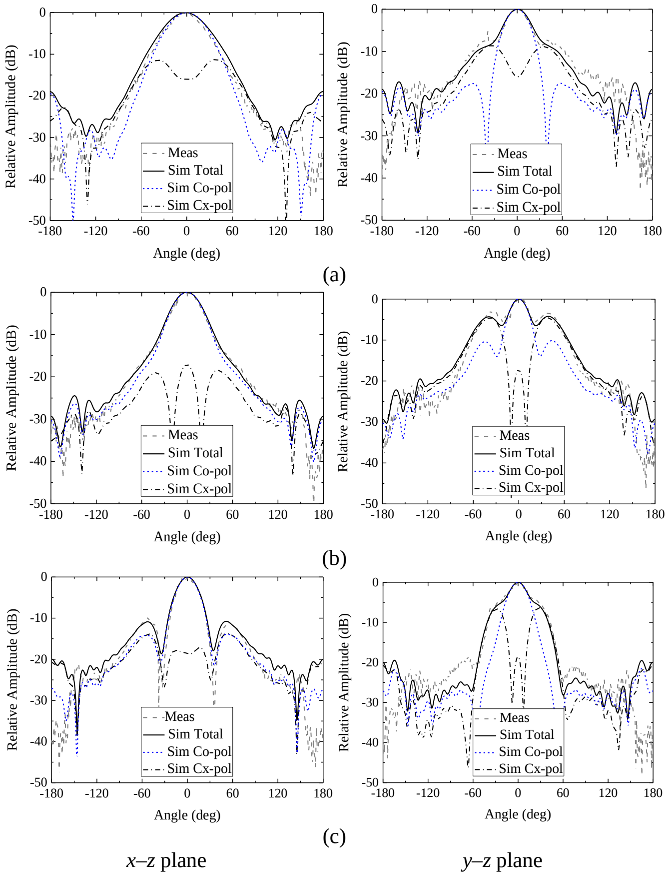

Fig. 9. Simulated and measured normalized radiation patterns of the proposed CP horn antenna. (a) f = 50 GHz. (b) f = 60 GHz. (c) f = 75 GHz.

All of the simulated results were solved by HFSS.

Fig. 8 illustrates and compares the measured and simulated reflection coefficients of the CP horn. The small frequency shift between simulation and experiment may be caused by the machining error. With reference to the figure, the simulated and measured -10 dB impedance bandwidths are 40% (50−75 GHz).

Fig. 9 illustrates and compares the measured and simulated normalized radiation patterns of the proposed antenna at frequencies of 50, 60 and 75 GHz. It should be noted that the sim total radiation pattern in Fig. 9 is the superposition of Co-pol (left hand circular polarization) and Cx-pol (right hand circular polarization) radiation pattern. In this communication's measurement setup to test the radiation pattern, the transmitting antenna is set as a horn antenna for horizontal and vertical polarization. The radiation pattern value is calculated by the superposition of these two measured results. With reference to Fig. 9, the simulated main beam of the total gain agrees well with the measured one. Within the range of half power beam width (HPBW), the simulated cross-polarization value are all less than -11 dB as given in Fig. 9. In this communication, the authors did not design the shape of the part of the circular waveguide surrounding the ATSA to enhance the radiation performance. This is beyond the scope of this communication and will be studied in the future. The asymmetry around the azimuth of ±170° is caused by the metal column on our rotary table. The AR and gain performances of the CP horn are presented in Fig. 10. The measured AR value is calculated by the ratio of horizontal and vertical polarization transmitting horn antenna. The lower measured AR results may be caused by the testing and machining errors. The simulated and

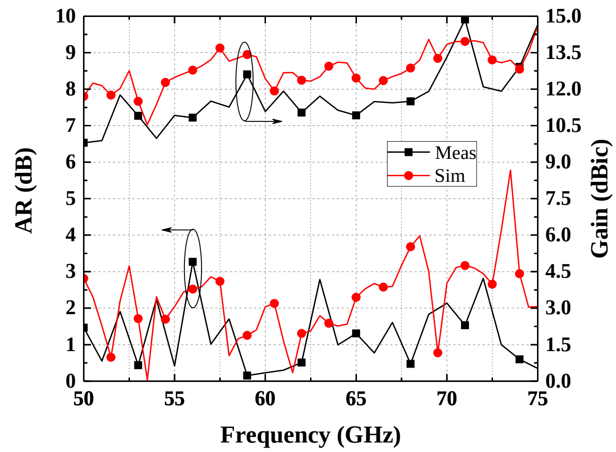

Fig. 10. The simulated and measured gain plots and AR plots of the proposed CP horn antenna.

measured AR bandwidths are 29.79% (50–67.5 GHz) and 40% for AR < 3.2 dB (50–75 GHz), respectively. The simulated and measured gains are also illustrated in Fig. 10. The diameter of circular waveguide of the proposed horn is larger than the standard circular waveguide, which excites the high order modes, and thus the gain plots is not smooth. As shown in Fig. 10, the simulated and measured results are 12.21± 2.4 dBic and 12.56± 2.02 dBic from 50 to 75 GHz, respectively.

IV. Conclusion

In this communication, a new type of wideband CP horn antenna was proposed and investigated. By inserting an ACTSA into a circular waveguide, the CP wave can be generated. The CP mechanism was explained in details. Moreover, a series of parameter studies were carried out to provide the guideline to readers for designing the proposed type of CP horn. Furthermore, a prototype was practically fabricated by EDM and measured by a millimeter-wave test system. The measured results indicate that the proposed antenna can achieve a bandwidth of 40% for both AR < 3.2 dB and S_{11} < -10 dB. Without OMT feeding, the proposed CP horn has a symmetrical radiation pattern in *x-z* and *y-z* plane, respectively, wide AR and impedance bandwidths as well as a simple structure. Therefore, in conclusion, the proposed antenna is a promising candidate for a millimeter-wave low-cost CP horn antenna. In the future, the authors will make further efforts on enhancing the radiation performance of the proposed type of horn antenna.

References

[1] K. Chang, *Handbook of Microwave and Optical Components, Microwave Passive and Antenna Components*. New York, NY, USA: Wiley, 1997, pp. 626–647.

[2] T. Manabe, K. Sato, H. Masuzawa, K. Taira, T. Ihara, Y. Kasashima,and K. Yamaki, "Polarization dependence of multipath propagation and highspeed transmission characteristics of indoor millimeter-wave channel at 60 GHz," *IEEE Trans. Veh. Technol*., vol. 44, no. 2, pp. 268-274, May. 1995.

[3] Y. Huang, J. Geng, R. Jin, X. Liang, X. Bai, X. Zhu, and C. Zhang, "A novel compact circularly polarized horn antenna," in *IEEE Antennas and Propagation Society International Symposium (APSURSI)*, July. 2014, pp. 43-44.

[4] N. Yoneda, M. Miyazaki, H. Matsumura, and M. Yamato, “A design of novel grooved circular waveguide polarizers,” *IEEE Trans. Microw. Theory Techn.*, vol. 48, no. 12, pp. 2446–2452, Dec. 2000.

[5] N. Yoneda, M. Miyazaki, T. Horie, and H. Satou, “Mono-grooved circular waveguide polarizers,” in *IEEE MTT-S Int. Microwave Symp. Dig.*, 2002, pp. 821–824.

[6] E. Lier and T. Schaug-Pettersen, “A novel type of waveguide polarizer with large cross-polar bandwidth,” *IEEE Trans. Microw. Theory Techn.*, vol. 36, pp. 1531–1534, Nov. 1988.

[7] S. W. Wang, C. H. Chien, C. L. Wang, and R. B. Wu, “A circular polarizer designed with a dielectric septum loading,” *IEEE Trans. Microw. Theory Techn.*, vol. 52, no.7, pp. 1719-1723, Jul. 2004

[8] Y. Tao, Z. Shen, and G. Liu, “Closed-form expressions for the equivalent circuit model of square-waveguide T-junctions and its application in ortho-mode transducer design,” *IEEE Trans. Microw. Theory Techn.*, vol. 58, no.5, pp. 1167-1174, May. 2010

[9] M. H. Chen and G. N. Tsandoulas, “A wide-band square waveguide array polarizer,” *IEEE Trans. Antennas Propag*., vol. AP-21, no. 3, pp. 389–391, May 1973.

[10] J. Bornemann and V. A. Labay, “Ridge waveguide polarizer with finite and stepped-thickness septum,” *IEEE Trans. Microw. Theory Techn.*, vol. MTT-43, pp. 1782–1787, Aug. 1995.

[11] N. C. Albertsen and P. Skov-Madsen, “A compact septum polarizer,” *IEEE Trans. Microw. Theory Techn.*, vol. MTT-31, pp. 654–660, Aug. 1983.

[12] Y. Cai, Y. Zhang, Z. Qian, W. Cao, and S. Shi, “Compact Wideband Dual Circularly Polarized Substrate Integrated Waveguide Horn Antenna,” *IEEE Trans. Antennas Propag.*, vol. 64, no. 7, pp. 3184–3189, Jul. 2016.

[13] Y. Yao, X. Cheng, J. Yu, and X. Chen, "Analysis and design of a novel circularly polarized antipodal linearly tapered slot antenna," *IEEE Trans. Antennas Propag*., vol. 64, no.10, pp. 4178-4187, Oct. 2016.

[14] Y. Yao, X. Cheng, J. Yu, and X. Chen, “Wideband circularly polarized antipodal curvedly tapered slot antenna array for 5G applications,” *IEEE J. Sel. Areas Commun*., vol .35, no. 7, Jul. 2017.

[15] Y. Liu, H. Lu, Y. Wu, M. Cui, B. Li, P. Zhao, and X. Lv, “Millimeterwave and terahertz waveguide-fed circularly polarized antipodal curvedly tapered slot antennas,” *IEEE Trans. Antennas Propag*., vol. 64, no.5, pp. 1607-1614, May. 2016.

[16] B. S. Guru and H. R. Hiziroglu, “Waveguide and cavity resonators,” in *Electromagnetic Field Theory Fundamentals*, 2nd ed. Cambridge, U.K.: Cambridge Univ. Press, 2004